

Incoherent Interplane Conductivity of κ -(BEDT-TTF)₂Cu[N(CN)₂]Br

J. J. McGuire, T. Rõm*, A. Pronin†, T. Timusk

Department of Physics and Astronomy, McMaster University, Hamilton, Ontario L8S 4M1, Canada

J. A. Schlueter, M. E. Kelly, A. M. Kini

Chemistry and Materials Science Divisions, Argonne National Laboratory, Argonne, Illinois 60439, USA

The interplane optical spectrum of the organic superconductor κ -(BEDT-TTF)₂Cu[N(CN)₂]Br was investigated in the frequency range from 40 to 40,000 cm⁻¹. The optical conductivity was obtained by Kramers-Kronig analysis of the reflectance. The absence of a Drude peak at low frequency is consistent with incoherent conductivity but in apparent contradiction to the metallic temperature dependence of the DC resistivity. We set an upper limit to the interplane transfer integral of $t_b^2/t_{ac} \approx 10^{-7}$ eV. A model of defect-assisted interplane transport can account for this discrepancy. We also assign the phonon lines in the conductivity to the asymmetric modes of the ET molecule.

PACS numbers: 74.25.Gz, 74.70.Kn, 78.30.Jw

Of the κ -type (BEDT-TTF)-based organic superconductors κ -(BEDT-TTF)₂Cu[N(CN)₂]Br has the highest superconducting transition temperature at ambient pressure,¹ $T_c = 12.5$ K. BEDT-TTF, or bis(ethylenedithio)tetrathiafulvalene and hereafter further abbreviated to ET, is a platelike molecule that, in the κ -type ET-based superconductors, forms conducting layers of orthogonally arranged dimers separated by insulating layers of anions.¹ The resulting quasi-two-dimensional electronic structure makes this class of organic superconductors of great interest due to their potential similarity to the high temperature cuprate superconductors.² One important issue is the nature of interlayer transport: is it coherent giving rise to a three dimensional Fermi liquid at sufficiently low temperature, or does it remain incoherent to the lowest temperatures? This issue is well illustrated by two two-dimensional superconductors, Sr₂RuO₄ which shows coherent interplane transport at low temperature and Bi₂Sr₂CaCu₂O_{8+δ} (Bi-2212) where the interplane transport is incoherent at all temperatures.

The first, Sr₂RuO₄, is isostructural with the cuprate superconductor La_{2-x}Sr_xCuO₄, and has a superconducting T_c of 1.5 K.³ Although highly anisotropic, it shows coherent interplane transport. At low temperature Sr₂RuO₄ shows metallic resistivity both in the in-plane and interplane directions, although the resistivity in the interplane direction is two orders of magnitude higher than that of the in-plane direction and has a metallic temperature dependence only below 100 K.³ The in-plane optical conductivity shows a Drude-like peak, and a weak Drude component can also be seen in the interlayer direction.^{4,5}

The cuprate superconductor Bi-2212 shows an in-plane DC resistivity that, in optimally doped Bi-2212, varies linearly with temperature up to several hundred Kelvin, while in the interplane direction the resistivity is four orders of magnitude higher and *increases* with decreasing temperature.^{6,7} The real part of the optical conductivity of Bi-2212 shows a Drude-like peak centred at zero frequency in the in-plane direction,⁸ but no such peak is

seen in the interplane direction.⁹ Instead, the interplane conductivity consists entirely of phonon lines. The weak residual interplane transport is due to an incoherent tunneling mechanism.⁶

The transport properties of κ -(ET)₂Cu[N(CN)₂]Br are also highly anisotropic.^{10,11} Within the conducting *ac*-planes, the resistivity shows an unusual broad peak near 100 K, but has a clearly metallic behaviour at low temperature with resistivity decreasing with decreasing temperature. The interplane *b*-axis resistivity has qualitatively the same metallic temperature dependence as the in-plane resistivity, but is three orders of magnitude higher. Its value of 1 Ωcm at 15 K, which depends somewhat on how quickly the sample is cooled,¹² is six orders of magnitude higher than what is seen in good metals. Thus, in the interplane direction, there is an apparent contradiction between the temperature dependence of the resistivity that suggests coherent transport, and the magnitude of the resistivity that suggests incoherent transport.

One criterion for evaluating the coherence of the interplane conductivity is the Ioffe-Regel-Mott minimum metallic conductivity. Modified for the open Fermi surfaces of these highly anisotropic systems,¹³ it gives a lower limit on conductivity which corresponds to a coherence length comparable to the size of a unit cell in the interlayer direction:

$$\sigma_{min} \approx \sqrt{\frac{\sigma_{\perp}}{\sigma_{\parallel}}} \frac{e^2}{2\pi^2\hbar} \frac{l_{\perp}}{l_{\parallel 1}l_{\parallel 2}} \quad (1)$$

where σ_{\perp} and l_{\perp} are the conductivity and lattice constant in the interplane direction and σ_{\parallel} , $l_{\parallel 1}$ and $l_{\parallel 2}$ are the conductivity and lattice constants in the planes. Table I lists these parameters for Sr₂RuO₄, Bi-2212 and κ -(ET)₂Cu[N(CN)₂]Br. The conductivity anisotropy ratio should be evaluated at $\sigma_{\perp} = \sigma_{min}$. For Sr₂RuO₄ this gives coherent conductivity below 52 K which is indeed the temperature where the resistivity starts to deviate from the low-temperature T^2 dependence. For Bi-2212 and κ -(ET)₂Cu[N(CN)₂]Br, however, $\sigma_{min} > \sigma_{\perp}$

TABLE I. Ioffe-Regel-Mott minimum metallic conductivity for highly anisotropic systems. $l_{\parallel 1}$, $l_{\parallel 2}$ and l_{\perp} are the two in-plane and one interplane room temperature lattice constants^{3,14,1} in Å, T is temperature in Kelvin, and σ_{\parallel} , σ_{\perp} and σ_{min} are the in-plane, interplane and minimum conductivities in $(\Omega\text{cm})^{-1}$ at temperature T .

	$l_{\parallel 1}$	$l_{\parallel 2}$	l_{\perp}	T	σ_{\parallel}	σ_{\perp}	σ_{min}
Sr_2RuO_4	3.9	3.9	12.7	52	28600	37	37
$\text{Bi}_2\text{Sr}_2\text{CaCu}_2\text{O}_{8+\delta}$	3.8	3.8	30.9	85	25000	0.17	3.4
$\kappa\text{-(ET)}_2\text{Cu[N(CN)}_2\text{]Br}$	12.9	8.5	30.0	12.5	1000	1	11

even near T_c where the anisotropy is largest. This suggests that the low temperature interplane conductivity of Sr_2RuO_4 is coherent but becomes incoherent above 52 K due to thermal fluctuations, while both Bi-2212 and $\kappa\text{-(ET)}_2\text{Cu[N(CN)}_2\text{]Br}$ remain incoherent at all temperatures.

Optical conductivity provides another method of investigating the coherence of interplane transport where in a coherent system the optical conductivity σ_1 shows a Drude peak centred at zero frequency with a maximum corresponding to the DC conductivity σ_{DC} and a width equal to the scattering rate Γ of the free carriers:

$$\sigma_1(\omega) = \frac{\sigma_{DC}\Gamma^2}{\omega^2 + \Gamma^2} \quad (2)$$

The question of the coherence of the interplane transport in the ET-based organic superconductors can be addressed with measurements of low temperature far-infrared optical conductivity in the interplane direction. To date however, infrared studies have focused on the in-plane properties,^{15–21} and the few interplane measurements which have been made^{22–25} were at room temperature and above 600 cm^{-1} . This is due to the difficulty of growing crystals with large faces perpendicular to the conducting planes. Recently, however, high quality crystals of sufficient size for far-infrared interplane measurements have become available. The interplane reflectance measurements of $\kappa\text{-(ET)}_2\text{Cu[N(CN)}_2\text{]Br}$ presented in this paper are the first such measurements on any ET based superconductor.

The single crystals of $\kappa\text{-(ET)}_2\text{Cu[N(CN)}_2\text{]Br}$ were synthesized by the electrocrystallization technique described elsewhere.¹ Typical crystal sizes were $1.5 \times 1.5 \times 1.5$ mm with faces as large as 1 mm^2 parallel to the interlayer b -axis. Polarized reflectance measurements between 40 and 8000 cm^{-1} were performed on these as-grown faces with a Michelson interferometer using three different detectors. A grating spectrometer with three additional detectors was used to make measurements at 300 K for the rest of the range up to 40,000 cm^{-1} (5 eV).

The reflectance of $\kappa\text{-(ET)}_2\text{Cu[N(CN)}_2\text{]Br}$ with the light polarized in the interplane direction is shown in Fig. 1 for four temperatures above the superconducting transition temperature. The reflectance is approximately

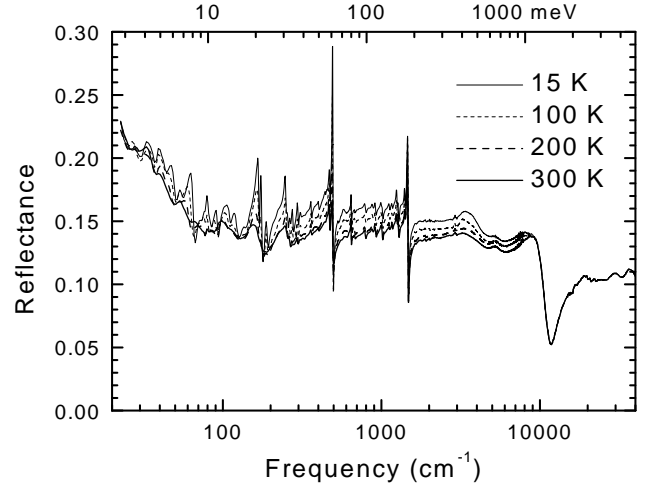


FIG. 1. Semilog plot of the interlayer reflectance of $\kappa\text{-(ET)}_2\text{Cu[N(CN)}_2\text{]Br}$.

0.15 over the entire range with several sharp phonon peaks at low frequencies and some broader interband-like features at higher frequencies.

It should also be pointed out that there was some sample-to-sample variation of the interplane reflectance, particularly the temperature dependence of the background reflectance above 200 cm^{-1} . Fig. 2 is a comparison of the sample shown in Fig. 1 (upper panel) with another sample showing a much stronger temperature dependence (lower panel). The phonon lines below 200 cm^{-1} also appear to be stronger in this second sample although the optical conductivity should be calculated for a true comparison. Unfortunately we were unable to measure reflectance above 800 cm^{-1} for this second sample, and we have no explanation for the variation. Complete data sets need to be collected on more samples to properly investigate this phenomenon. It is interesting to note that the feature has the appearance of a gap, and evidence for a pseudogap in $\kappa\text{-(ET)}_2\text{Cu[N(CN)}_2\text{]Br}$ at $T^* = 50$ K in ESR²⁶ and ^{13}C NMR^{27,28} measurements has been reported. This would give $2\Delta/k_B T^* = 5.7$ which is not far from the value 4.3 reported for the high temperature cuprate superconductors.²⁹

The calculation of the optical conductivity requires extrapolation of the reflectance to all frequencies for the Kramers-Kronig analysis. The spectra were extrapolated to high frequencies using power law extrapolations: ω^{-1} above 5 eV and ω^{-4} above 62 eV. Below our lowest measured point at 25 cm^{-1} we used a Drude extrapolation, although an insulating extrapolation gives very similar results. We estimate our experimental uncertainty of the reflectance to be ± 0.005 . Combined with uncertainties due to the extrapolations, this gives an uncertainty in our optical conductivity of $\pm 8\%$ between 200 and 2000 cm^{-1} . Outside this range the uncertainty rises, reaching $\pm 40\%$ at 25 and 5000 cm^{-1} . The resolution of the spectra is

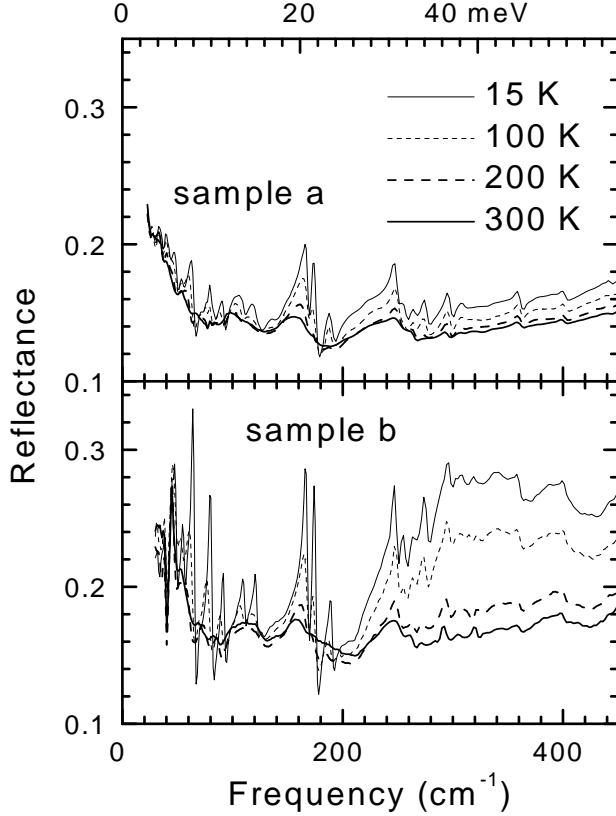


FIG. 2. A comparison of the interlayer reflectance of two crystals of κ -(ET) $_2$ Cu[N(CN) $_2$]Br. The one in the lower panel shows stronger temperature dependence of the background above 200 cm^{-1} .

2 cm^{-1} up to 200 cm^{-1} , 4 cm^{-1} up to 680 cm^{-1} , and 15 cm^{-1} up to 8000 cm^{-1} .

The real part of the interplane optical conductivity is shown in Fig. 3. The value of the DC conductivity from the work of Su *et al.*¹² at 15 K is shown at 1 (Ωcm) $^{-1}$ on the vertical axis. Clearly there is no sign of the usual Drude peak that accompanies coherent conductivity. Instead the conductivity is dominated by sharp phonon lines on a background due to interband-like features in the mid-infrared. This confirms that the interlayer conductivity in κ -(ET) $_2$ Cu[N(CN) $_2$]Br is incoherent.

A fit to Lorentz oscillators which will be discussed later shows no sign of any free carrier component to the optical conductivity above 30 cm^{-1} . This is similar to what has been reported for Bi-2212.⁹ It is difficult to estimate an upper limit for the plasma frequency of a hypothetical Drude peak, but assuming the width is equal to the in-plane width reported by Eldridge and Kornelsen of $\Gamma = 20 \text{ cm}^{-1}$ we estimate $\omega_p = 50 \text{ cm}^{-1}$ for the plasma frequency of the Drude component. Combining the in-plane scattering rate $\Gamma = 20 \text{ cm}^{-1}$ with the DC resistivity gives a somewhat lower value of $\omega_p = 25 \text{ cm}^{-1}$. Using the 50 cm^{-1} value and a simplified tight-binding model

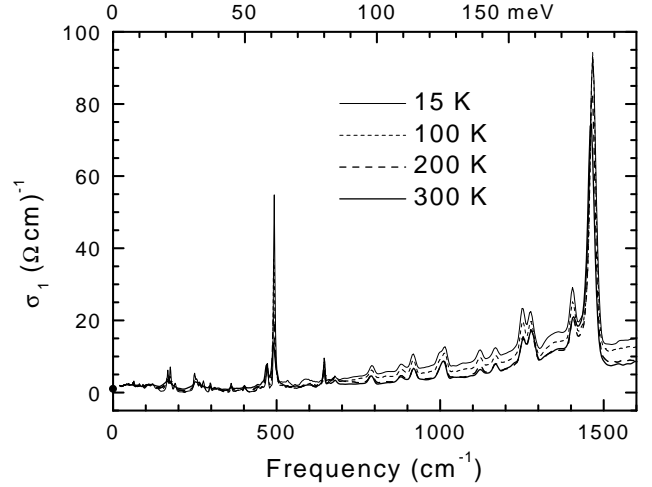


FIG. 3. The real part of the interlayer optical conductivity of κ -(ET) $_2$ Cu[N(CN) $_2$]Br. The DC value is marked on the vertical axis at 1 (Ωcm) $^{-1}$.

we can estimate the interplane transfer integral using²¹

$$\omega_p^2 = \frac{e^2}{\epsilon_0 \hbar^2} \sum_{BZ} f(E_{\mathbf{k}}) \frac{\partial^2 E}{\partial k_\mu^2} \quad (3)$$

where $f(E_{\mathbf{k}})$ is the Fermi-Dirac occupation number and the derivative is to be taken in the direction of the field. We use the simplified tight-binding band

$$E_{\mathbf{k}} = -2t_a \cos(k_a d_a) - 2t_b \cos(k_b d_b) - 2t_c \cos(k_c d_c) \quad (4)$$

where d are the ET molecular repeat distances and t are the average transfer integrals along the various directions. We assume an open Fermi surface in the interplane direction³⁰ with $t_b \ll t_{ac}$ and ignore the in-plane anisotropy to get

$$\omega_{pb} \approx \frac{e^2}{\epsilon_0 \hbar^2} \frac{b^2/V_m}{\sqrt{\pi} \sin(\sqrt{\pi})} \frac{t_b^2}{t_{ac}} \quad (5)$$

where b is the interplane lattice constant and V_m the volume per ET molecule. This gives $t_b^2/t_{ac} \approx 10^{-7} \text{ eV}$ which gives $t_b \approx 10^{-4} \text{ eV}$ if $t_{ac} \approx 10^{-1} \text{ eV}$ as has been estimated for (ET) $_2$ I $_3$.²¹ Of course, this analysis assumes a coherent component to the conductivity which seems unlikely given the earlier discussion of minimum metallic conductivity.

We now return to the problem of the temperature dependence of the interplane DC conductivity which shows a clear metallic character and in fact follows rather accurately the in-plane conductivity although it is a factor of 1000 smaller. Since the interplane conductivity is below the minimum metallic limit it is highly likely that its metallic temperature dependence is due to some special process that makes it mirror the in-plane conductivity. There are several models that can do this^{31,32} and we

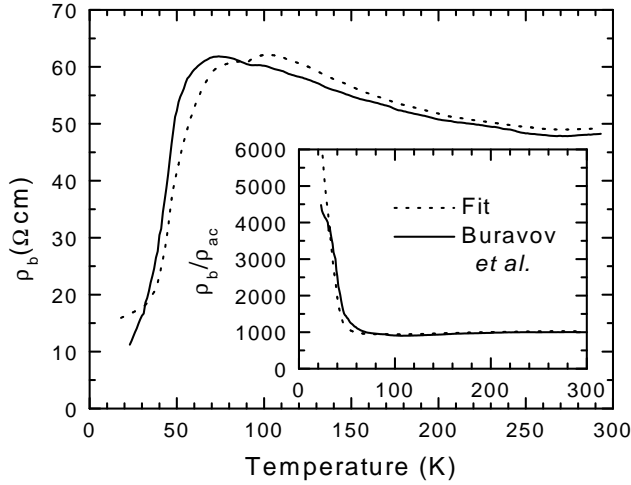


FIG. 4. A comparison of the resistivity data of Buravov *et al.*¹⁰ to a fit to the model of Martin *et al.*⁷

focus here on a model originally proposed for Bi-2212 by Martin *et al.*,⁷ where the conducting planes are connected by a random network of shorts approximated as a regular array of links of resistance R_{lb} distance ξ apart along the conducting plane. Given the resistance R_{lac} along the plane between the shorts and the interplane distance d , the apparent interplane resistivity is given by

$$\rho_b = (R_{lb} + R_{lac}) \times \frac{(\xi/2)^2}{d} \quad (6)$$

and assuming $R_{lac} = \rho_{ac}/d$ we get for the anisotropy

$$\frac{\rho_b}{\rho_{ac}} = \left(1 + \frac{dR_{lb}}{\rho_{ac}}\right) \times \left(\frac{\xi}{2d}\right)^2 \quad (7)$$

Buravov's data¹⁰ above 50 K are nearly temperature-independent with $\rho_b/\rho_{ac} \approx 1000$, while below 50 K the anisotropy rises dramatically. Fig. 4 compares the interplane resistivity and anisotropy of Buravov *et al.* with a least squares fit using Eq. 7 assuming a temperature-independent R_{lb} . The fit, which reproduces both the temperature independence of the anisotropy at high temperatures and the dramatic increase in anisotropy at low temperatures, gives $R_{lb} = 138 \pm 9 \text{ k}\Omega$ and $\xi = 802 \pm 7 \text{ \AA}$ if we take $d = 15 \text{ \AA}$. The model explains the rise of the anisotropy below 50 K as due to the rapid drop of R_{lac} relative to the temperature-independent R_{lb} , whereas models where the proportionality between in-plane and interplane resistivity is built in^{31,32} predict a constant anisotropy, independent of temperature. The observed sample-to-sample variation shown in Fig. 2 is also consistent with a process controlled by defects.

The model of a meandering current will fail at high frequency. To estimate the characteristic maximum frequency we model the current path as a transmission line of series resistors R_{lac} shunted to ground by capacitors

C_s where we set $C_s \approx 2\pi\xi$. The impedance of such a transmission line is

$$Z = \frac{R_{lac}}{2} \left(1 + \sqrt{1 + \frac{4i}{\omega R_{lac} C_s}}\right) \quad (8)$$

Thus above a frequency given by $\omega_0 = (R_{lac} C_s)^{-1}$ the capacitors short the AC current and the in-plane fields do not have time to build up. With the parameters determined above we find that $\omega_0 \approx 10 \text{ cm}^{-1}$. A test of the model would be a reduction of the interplane conductivity from its DC value to a much lower value at this frequency. Dressel *et al.*¹¹ find in the millimeter wave range (1-3 cm^{-1}) conductivities that agree with DC values consistent with our picture. Unfortunately the strong phonon background discussed in the next paragraphs prevents us from giving an accurate value of the interplane electronic conductivity in the far infrared range other than an upper limit of about $1 (\Omega\text{cm})^{-1}$.

It was possible to fit the conductivity with a series of Lorentzian oscillators according to

$$\sigma_1(\omega) = \frac{1}{4\pi} \sum_i \frac{\omega_{pi}^2 \omega^2 \Gamma_i}{(\omega_{0i}^2 - \omega^2)^2 + \omega^2 \Gamma_i^2} \quad (9)$$

51 oscillators were used in the fit along with a weak Drude term to account for phonons below the measurement range and one strong oscillator at high frequency to provide the background tail of the mid-infrared features. It was necessary to add some asymmetry to the strongest oscillators at 492 and 1450 cm^{-1} , but all other oscillators were symmetric. Table II lists the frequency ω_0 , plasma frequency ω_p and width Γ of the oscillators at all four temperatures. Most of the low frequency lines seem to be lattice modes as their frequencies increase with decreasing temperature.³³ Some of these lines were previously reported in a powder absorption experiment³³ and are marked with an asterisk. The rest of the lines are related to internal vibrations of the ET molecule, and these mode assignments were made by comparison with Eldridge *et al.* who assign the normal modes of the ET molecule³⁴ and relate these ET modes to observed lines in in-plane infrared and Raman spectra of $\kappa\text{-(ET)}_2\text{Cu[N(CN)}_2\text{]Br}$.^{35,36}

In general, infrared spectra are sensitive to asymmetric (ungerade) modes while Raman spectra are sensitive to symmetric (gerade) modes. Since the ET molecule consists of two mirrored halves joined by a single C=C bond, the infrared and Raman spectra of ET contain similar sets of lines.³⁴ Each vibration of atoms in one half of the molecule can be in phase or out of phase with an identical vibration in the other half producing symmetric/asymmetric pairs of modes. Since the two halves are nearly independent, the members of each mode pair have nearly the same energy. This argument does not apply to modes involving the central C=C bond.

Like the ET spectra, the in-plane infrared and Raman spectra of $\kappa\text{-(ET)}_2\text{Cu[N(CN)}_2\text{]Br}$ also have similar sets of lines, however in this case both sets of lines

TABLE II. Lorentz oscillator parameters from least squares fits of Eq. (9) to the real part of the interplane optical conductivity of κ -(ET)₂Cu[N(CN)₂]Br at 15, 100, 200 and 300 K. All values are in cm⁻¹. Vertical lines associate one or more mode assignments with a set of oscillators. * indicate lines seen by Dressel *et al.*³³

	15 K			100 K			200 K			300 K		
	ω_0	ω_p	Γ	ω_0	ω_p	Γ	ω_0	ω_p	Γ	ω_0	ω_p	Γ
	28.4	4.3	1.9	27.9	5.7	2.4	29.4	7.6	4.0	29.2	5.5	3.9
	34.4	15.3	5.8	34.5	15.7	6.4	34.6	17.1	7.2	34.0	17.2	7.2
	41.3	21.8	7.5	41.0	19.0	6.8	40.9	15.0	5.9	41.1	18.1	9.3
*	47.9	19.2	5.6	47.0	21.5	7.7	46.1	21.9	8.9	46.3	19.8	11.5
*	55.5	25.4	10.8	54.7	21.5	9.6	53.9	18.8	9.5	54.6	20.2	10.9
*	63.5	27.3	5.7	61.6	27.7	7.6	59.6	23.6	8.6	59.6	20.0	12.4
	72.0	12.4	4.4	71.4	19.1	8.4	69.9	27.2	14.4	69.5	28.5	15.4
	75.7	5.0	2.1	75.8	8.1	2.7	75.4	13.0	6.0	75.3	8.5	5.1
*	81.2	30.2	8.9	80.2	23.3	8.0	80.4	8.5	3.8	80.3	5.4	2.5
*	91.3	20.7	5.1	89.5	23.1	8.2	86.7	25.1	12.8	84.8	17.6	10.5
	103.0	21.8	9.4									
*	109.1	24.7	7.6	106.3	31.0	12.3	103.7	18.6	9.7			
*	121.2	39.8	13.3	118.9	30.4	15.8	113.4	35.3	27.8			
	136.5	14.7	7.1									
*	167.1	39.7	4.6	166.1	47.2	9.5	165.0	52.1	17.3			
*	175.3	42.9	4.7	175.1	37.7	7.5	175.9	35.1	14.9			
*	190.0	27.7	5.5	190.0	27.2	7.4	189.2	22.0	11.8			
*	248.7	39.0	5.3	249.7	23.7	4.9	251.4	30.6	8.9			
*	255.9	39.2	8.6	253.2	51.5	15.2						
$\nu_{53}(\text{B}_{2u})$	265.6	21.8	5.6	265.7	17.1	4.9	265.0	19.2	6.2			
$\nu_{36}(\text{B}_{1u})$ *	276.3	32.0	5.8	275.8	29.3	6.8	275.5	22.0	9.8			
*	297.7	24.0	3.1	297.6	21.4	3.5	296.7	20.0	4.8	295.3	20.0	7.7
	311.1	22.1	8.0	311.7	16.6	7.0	310.2	10.5	5.1	308.5	14.0	8.6
	325.5	33.3	26.5	321.9	23.3	13.7	324.6	29.9	30.0	321.5	24.1	18.2
$\nu_{52}(\text{B}_{2u})$	360.9	27.6	5.2	361.6	20.2	3.8	361.6	22.5	6.5	361.6	16.4	5.9
$\nu_{35}(\text{B}_{1u})$	402.2	28.2	7.6	402.6	21.9	6.3	402.3	19.6	6.8	401.4	17.2	7.2
$\nu_{34}(\text{B}_{1u})$	471.3	57.8	6.4	471.1	58.6	7.5	470.3	63.9	9.6	469.4	65.4	11.4
	492.1	125.5	4.6	491.3	112.7	5.2	490.4	101.9	8.0	489.8	94.3	12.0
$\nu_{33}(\text{B}_{1u})$	595.3	91.8	54.2	598.9	68.7	48.0	596.9	63.0	54.0	595.3	33.2	25.1
$\nu_{51}(\text{B}_{2u})$	645.8	48.6	5.2	645.8	48.1	5.6	644.8	48.1	6.4	644.1	44.9	6.9
$\nu_{50}(\text{B}_{2u})$	676.5	68.5	40.7	677.8	68.8	33.6	676.7	63.8	28.5	677.5	37.4	19.0
$\nu_{32}(\text{B}_{1u})$	791.2	73.8	23.4	790.5	62.7	21.5	790.0	61.6	21.0	788.9	53.4	17.4
$\nu_{15}(\text{A}_u)$	837.7	105.0	61.2	837.4	85.8	56.2	836.1	63.4	49.3	839.2	38.2	34.6
$\nu_{49}(\text{B}_{2u})$	881.9	92.2	34.5	881.9	83.4	31.9	881.0	69.1	28.3	879.4	63.9	29.5
$\nu_{48}(\text{B}_{2u})$	917.2	92.1	22.0	917.8	85.0	20.4	919.1	75.9	20.0	919.0	73.8	20.5
$\nu_{31}(\text{B}_{1u})$												
$\nu_{30}(\text{B}_{1u})$	998.7	93.7	28.3	999.6	83.4	27.3	1001.7	78.0	27.5	1002.8	78.3	24.2
$\nu_{47}(\text{B}_{2u})$	1015.4	78.6	17.8	1015.0	76.4	17.6	1013.7	61.1	16.0	1012.8	51.3	13.1
$\nu_{14}(\text{A}_u)$	1121.8	103.9	31.9	1122.2	97.5	31.8	1122.2	78.1	27.6	1123.2	83.1	38.5
$\nu_{67}(\text{B}_{3u})$	1167.3	113.3	36.3	1168.9	104.9	36.3	1168.6	78.6	27.2	1168.3	76.1	25.5
$\nu_{46}(\text{B}_{2u})$	1251.3	132.3	21.1	1251.7	119.3	20.3	1252.5	100.9	19.8	1253.0	98.0	21.2
$\nu_{29}(\text{B}_{1u})$	1277.3	138.2	24.6	1278.2	131.3	24.1	1278.9	130.1	24.6	1279.4	131.1	26.2
$\nu_{28}(\text{B}_{1u})$	1404.4	134.7	19.2	1405.4	133.9	21.2	1406.1	129.4	24.3	1406.9	123.0	24.6
$\nu_{45}(\text{B}_{2u})$												
$\nu_{27}(\text{B}_{1u})$	1467.7	343.9	22.9	1467.3	325.0	19.9	1465.5	316.9	20.8	1462.5	321.1	24.0
$\nu_{26}(\text{B}_{1u})$	2921.0	62.7	17.8	2920.4	60.9	18.1	2922.4	55.0	18.7	2920.4	52.0	20.2
	2938.6	53.7	24.0	2937.4	49.4	25.0	2938.9	48.7	24.4	2939.6	48.6	26.0
$\nu_{44}(\text{B}_{2u})$	2960.5	52.5	20.2	2960.8	58.0	24.9	2963.1	54.5	23.2	2962.8	51.4	20.2
$\nu_{66}(\text{B}_{3u})$	2982.4	44.5	13.6	2983.2	46.1	15.6	2982.0	38.6	18.1	2981.3	48.3	24.9

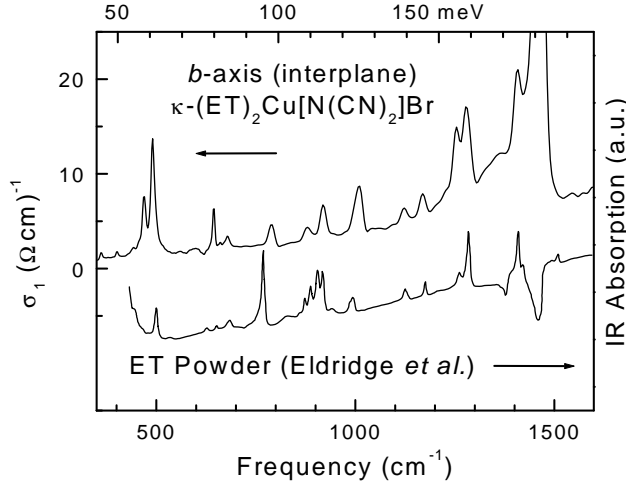


FIG. 5. A comparison at 300 K of the real part of the interlayer optical conductivity with the powder absorption spectra of Eldridge *et al.*³⁴

are ascribed to the symmetric modes of ET.³⁵ The reason the symmetric ET modes are infrared-active in κ -(ET)₂Cu[N(CN)₂]Br is the arrangement of ET molecules into dimers so that the members of a dimer can vibrate out of phase transferring charge back and forth and producing the dipole moment required for infrared activity. The Raman line positions in κ -(ET)₂Cu[N(CN)₂]Br are shifted from the ET line positions due to the charge on the ET molecules, and the infrared line positions are further shifted by their coupling to the charge transfer between members of a dimer.³⁵ To assist them in their mode assignments, Eldridge *et al.* also cause further shifts using several isotopic substitutions.

We have assigned the lines in our interplane infrared spectra to the asymmetric modes of the ET molecule. The mechanism that makes the symmetric modes infrared-active in the in-plane measurements does not apply to our interplane measurements since the electric vector of the light is perpendicular to the direction of charge transfer between members of a dimer. Fig. 5 shows a comparison of our σ_1 to the ET powder absorption spectrum of Eldridge *et al.*³⁴ For the most part, our mode assignments are based on this comparison since we do not have many measurements on isotopic analogs to assist us. We do however have a partial reflectance spectrum of a κ -(¹³C(2)-ET)₂Cu[N(CN)₂]Br crystal in which the two central carbon atoms have been substituted with ¹³C. Fig. 6 shows the 23 cm⁻¹ shift of a line at 791.2 cm⁻¹ confirming its identity as the ν_{32} (B_{1u}) mode.³⁴ Since this mode involves the central C=C bond, its symmetric counterpart is at a very different frequency and is seen in the in-plane infrared and Raman spectra near 450 cm⁻¹ while no line is seen near 791 cm⁻¹.³⁵

In general, all of the lines become narrower as temperature decreases as expected, however the plasma fre-

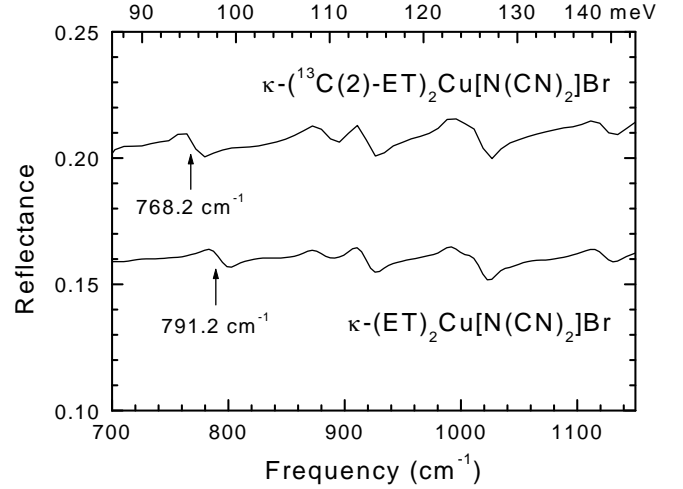


FIG. 6. A comparison at 15 K of the interlayer reflectance of κ -(ET)₂Cu[N(CN)₂]Br with that of a sample in which the two central carbon atoms have been substituted with ¹³C.

quencies, or line strengths, also increase significantly in some cases. In particular, the line at 81 cm⁻¹, which is quite strong at 15 K, has nearly disappeared above 200 K. An increase in line strength with decreasing temperature in organic conductors has generally been interpreted as a signature of charge-density-wave fluctuations.^{37,38} However, temperature-dependent phonon intensities have also been associated with spin-density-wave transitions.³⁹

In summary we have measured the interplane reflectance of the quasi-two-dimensional organic superconductor κ -(ET)₂Cu[N(CN)₂]Br and calculated the optical conductivity using Kramers-Kronig relations. We find strong evidence of incoherent transport as has been reported for the high temperature superconductors, and estimate an upper limit for the free carrier plasma frequency of 50 cm⁻¹ from which we derive an upper limit for the interplane transfer integral of 10⁻⁴ eV. We have used a defect model to explain the crossover from a temperature-independent resistivity anisotropy at high temperatures to a rapidly increasing anisotropy at low temperatures. We have also fit the phonon lines in the conductivity to a series of Lorentzian oscillators and assigned these to the asymmetric modes of the ET molecule.

The work at McMaster University was supported by the Natural Sciences and Engineering Research Council of Canada. Work at Argonne National Laboratory is sponsored by the U.S. Department of Energy, Office of Basic Energy Sciences, Division of Materials Sciences, under Contract W-31-109-ENG-38.

- * Permanent address: National Institute of Chemical Physics and Biophysics, Akadeemia tee 23, Tallinn 12618, Estonia.
- † New address: Institute of General Physics, Russian Academy of Sciences, 38 Vavilov str., 117942 Moscow, Russia.
- ¹ A.M. Kini, U. Geiser, H.H. Wang, K.D. Carlson, J.M. Williams, W.K. Kwok, K.G. Vandervoort, J.E. Thompson, D.L. Stupka, D. Jung, and M.H. Whangbo, *Inorg. Chem.* **29**, 2555 (1990).
 - ² R.H. McKenzie, *Science* **278**, 820 (1997), cond-mat/9812113.
 - ³ Y. Maeno, H. Hashimoto, K. Yoshida, S. Nishizaki, T. Fujita, J.G. Bednorz, and F. Lichtenberg, *Nature (London)* **372**, 532 (1994).
 - ⁴ T. Katsufuji, M. Kasai, and Y. Tokura, *Phys. Rev. Lett.* **76**, 126 (1996).
 - ⁵ M.G. Hildebrand, M. Reedyk, T. Katsufuji, and Y. Tokura, to be published.
 - ⁶ T. Watanabe and A. Matsuda, *Phys. Rev. B* **54**, R6881 (1996).
 - ⁷ S. Martin, A.T. Fiory, R.M. Fleming, L.F. Schneemeyer, and J.V. Waszczak, *Phys. Rev. Lett.* **60**, 2194, 1988.
 - ⁸ M.A. Quijada, D.B. Tanner, R.J. Kelley, M. Onellion, H. Berger, and G. Margaritondo, *Phys. Rev. B* **60**, 14917 (1999).
 - ⁹ S. Tajima, G.D. Gu, S. Miyamoto, A. Odagawa, and N. Koshizuka, *Phys. Rev. B* **48**, 16164 (1993).
 - ¹⁰ L.I. Buravov, N.D. Kushch, V.A. Merzhanov, M.V. Osheerov, A.G. Khomenko, and E.B. Yagubskii, *J. Phys. I France* **2**, 1257 (1992).
 - ¹¹ M. Dressel, O. Klein, G. Grüner, K.D. Carlson, H.H. Wang, and J.M. Williams, *Phys. Rev. B* **50**, 13603 (1994).
 - ¹² X. Su, F. Zuo, J.A. Schlueter, M.E. Kelly, and J.M. Williams, *Phys. Rev. B* **57**, R14056 (1998).
 - ¹³ Y.B. Xie, *Phys. Rev. B* **45**, 11375 (1992).
 - ¹⁴ R.M. Hazen, in *Physical Properties of High Temperature Superconductors II*, edited by D.M. Ginsberg (World Scientific, Singapore, 1990), p. 168.
 - ¹⁵ J.E. Eldridge, K. Kornelsen, H.H. Wang, J.M. Williams, A.V. Strieby Crouch, and D.M. Watkins, *Solid State Commun.* **79**, 583 (1991).
 - ¹⁶ T. Sugano, H. Hayashi, M. Kinoshita, and K. Nishikida, *Phys. Rev. B* **39**, 11387 (1989).
 - ¹⁷ K. Kornelsen, J.E. Eldridge, H.H. Wang, and J.M. Williams, *Phys. Rev. B* **44**, 5235 (1991).
 - ¹⁸ K. Kornelsen, J.E. Eldridge, H.H. Wang, H.A. Charlier, and J.M. Williams, *Solid State Commun.* **81**, 343 (1992).
 - ¹⁹ M. Meneghetti, R. Bozio, and C. Pecile, *J. Phys.* **47**, 1377 (1986).
 - ²⁰ M.G. Kaplunov, E.B. Yagubskii, L.P. Rosenberg, and Y.G. Borodko, *Phys. Stat. Solidi (a)* **89**, 509 (1985).
 - ²¹ C.S. Jacobsen, J.M. Williams, and H.H. Wang, *Solid State Commun.* **54**, 937 (1985).
 - ²² M. Tokumoto, H. Anzai, K. Takahashi, N. Kinoshita, K. Murata, T. Ishiguro, Y. Tanaka, Y. Hayakawa, H. Nagamori, and K. Nagasaka, *Syn. Metals* **27**, A171 (1988).
 - ²³ R.M. Vlasova, S.Y. Prieve, V.N. Semkin, R.N. Lyubovskaya, E.I. Zhilyaeva, and V.M. Yartsev, *Mater. Sci.* **17**, 75 (1991).
 - ²⁴ R.M. Vlasova, S.Y. Prieve, V.N. Semkin, R.N. Lyubovskaya, E.I. Zhilyaeva, E.B. Yagubskii, and V.M. Yartsev, *Syn. Metals* **48**, 129 (1992).
 - ²⁵ R.M. Vlasova, O.O. Drozdova, V.N. Semkin, N.D. Kushch, and E.B. Yagubskii, *Phys. Solid State* **35**, 408 (1993).
 - ²⁶ V. Kataev, G. Winkel, D. Khomskii, D. Wohlleben, W. Crump, K.F. Tebbe, and J. Hahn, *Solid State Commun.* **83**, 435 (1992).
 - ²⁷ H. Mayaffre, P. Wzietek, C. Lenoir, D. Jérôme, and P. Batail, *Europhys. Lett.* **28**, 205 (1994).
 - ²⁸ A. Kawamoto, K. Miyagawa, Y. Nakazawa, and K. Kanoda, *Phys. Rev. Lett.* **74**, 3455 (1995).
 - ²⁹ T. Nakano, N. Momono, M. Oda, and M. Ido, *J. Phys. Soc. Japan* **67**, 2622 (1998).
 - ³⁰ C.S. Jacobsen, D.B. Tanner, and K. Bechgaard, *Phys. Rev. B* **28**, 7019 (1983).
 - ³¹ N. Kumar and A.M. Jayannavar, *Phys. Rev. B* **45**, 5001 (1992).
 - ³² L. Forro, V. Ilakovac, J.R. Cooper, C. Ayache, and J.-Y. Henry, *Phys. Rev. B* **46**, 6626 (1992).
 - ³³ M. Dressel, J.E. Eldridge, J.M. Williams, and H.H. Wang, *Physica C* **203**, 247 (1992).
 - ³⁴ J.E. Eldridge, C.C. Homes, J.M. Williams, A.M. Kini, and H.H. Wang, *Spectrochimica Acta* **51A**, 947 (1995).
 - ³⁵ J.E. Eldridge, Y. Xie, H.H. Wang, J.M. Williams, A.M. Kini, and J.A. Schlueter, *Spectrochimica Acta* **52A**, 45 (1996).
 - ³⁶ J.E. Eldridge, Y. Xie, H.H. Wang, J.M. Williams, A.M. Kini, and J.A. Schlueter, *Mol. Cryst. Liq. Cryst.* **284**, 97 (1996).
 - ³⁷ M.J. Rice, *Phys. Rev. Lett.* **37**, 36, (1976).
 - ³⁸ M.J. Rice, L. Pietronero and P. Bruesch, *Solid State Commun.* **21**, 757 (1977).
 - ³⁹ H.K. Ng, T. Timusk, and K. Bechgaard, *Phys. Rev. B* **30**, 5842 (1984).